

## NUMERICAL MODELING OF AN OUTOKUMPU FLOTATION DEVICE

Juha TIITINEN<sup>1</sup>, Jussi VAARNO<sup>2</sup> and Sami GRÖNSTRAND<sup>3</sup>

<sup>1</sup> Helsinki University of Technology, Mechanical Process Technology and Recycling  
P.O.Box 6200, FIN-02015 HUT, Finland

<sup>2</sup> Outokumpu Research OY, P.O. Box 60 FIN-28101 Pori, Finland

<sup>3</sup> Outokumpu Technology – Minerals Processing, Riihitontuntie 7C FIN-02200 Espoo, Finland

### ABSTRACT

This paper reviews the detailed hydrodynamics of Outokumpu flotation cells by using CFD modeling.

Scope of this work was to build an industrial tool, based on CFD, for modeling flow field and solids distribution in flotation cell without air feed. Selection of tested and validated fundamental methods for achieving optimal cycle for analysis was also objective. Preprocessing, solver time and postprocessing for testing design layout with CFD should be done in less than one week.

The combination of basic approaches was chosen by simulating the single phase (*l*) flow field in process and laboratory scale flotation cells with different type and size computational grids and principal methods. Comparisons between velocity and turbulence results measured using the LDV (Laser Doppler Velocimetry) technique and CFD modeling were done. Also mixing power and liquid phase mixing time calculations were compared to validating measurements.

### INTRODUCTION

Froth flotation is a complex three phase physico-chemical process which is used in mineral processing industry to separate selectively fine valuable minerals from gangue. Main functions for flotation machines are to keep mineral grains in suspension and disperse sufficient amount of fine airbubbles to the pulp, energy efficiency and low power and air consumption

The flotation cell by Outokumpu in general consists of flotation tank, rotor and stator, air feed mechanism and pulp feed- and discharge mechanism. Figure 1 shows Outokumpu cell design in general. Industrial cell size can be from 5m<sup>3</sup> to 200m<sup>3</sup>. Figure 2 is a close up demonstration of air distribution and slurry pumping. The Outokumpu's rotor profile was originally designed to equilibrate the hydrodynamic and static pressures, allowing a uniform air dispersion over surface of the blades. The blade design also provides separate zones for air distribution and slurry pumping.

Development of flotation machines has earlier mainly been build on experimental data or rules of thumb. Now a Computational Fluid Dynamic (CFD) based tool for design and study of flotation cells is under development.

### ROLE OF GRID TYPE

Mesh generation is a significant part of CFD modeling. Mesh generation consumes most of the total time used to analysis. Moreover, the quality of the computed solution is substantially dependent on the structure and quality of the computational mesh. The attributes associated with mesh quality are node point distribution, smoothness and skewness. Building a valid computational mesh is a separate species of science which can be separated to structured and unstructured grid generation.

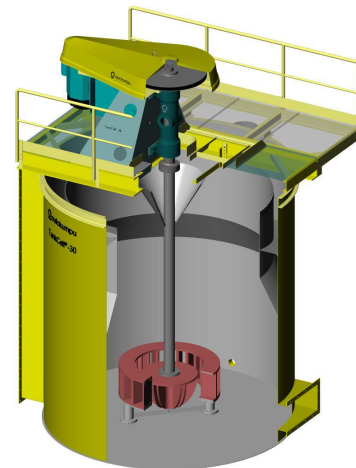


Figure 1: Outokumpu Flotation Cell.

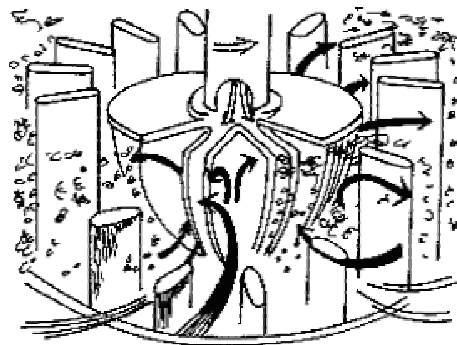


Figure 2: Rotor-stator close up.

Choosing appropriate mesh type will mainly depend on the geometry of the flow problem. Figure 3 shows general 3D grid cells types accepted by most of the CFD solvers.

Figure 4 shows an example of 3D multiblock structured grid and unstructured tetrahedral grid.

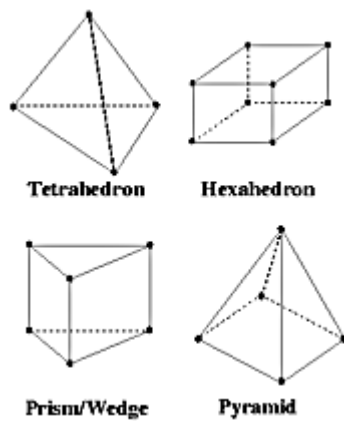


Figure 3: 3D Cell types.

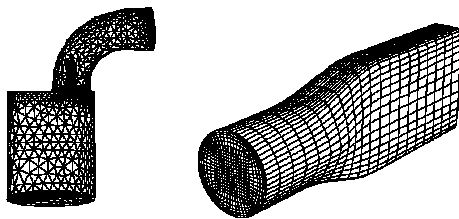


Figure 4: Grid topologies.

When choosing appropriate mesh type for flow problem there are some issues to consider:

Many flow problems involve complex geometries. The creation of a structured mesh for such geometries can be substantially time-consuming and perhaps for some geometries impossible. **Preprocessing time** is the main motivation for using unstructured mesh in these geometries.

**Computational expense** can be a determinant factor when geometries are complex or the range of length scales of the flow is large. Hexahedral elements generally fill more efficiently computational volume than tetrahedral elements.

A dominant source of error in calculations is **numerical diffusion**. Amount of numerical diffusion is inversely related to the resolution of the mesh. Also numerical diffusion is minimized when the flow is aligned with the mesh. In unstructured mesh cases with tetrahedral elements the flow can never be aligned with the grid.

Using and combining different types of elements as a hybrid mesh can be a good option and bring considerable flexibility in mesh generation.

#### GRID TYPE DEPENDENCY AND MIXING TIME

The grid type dependency calculations were carried out with an industrial size Outokumpu flotation tank cell. The geometrical details of the tank are given in Table 1. Geometry is rotationally symmetric and therefore it was sufficient to model only a part of the domain. The smallest symmetry of the geometry is 60° which contains one impeller blade and three stator blades. Two different type of grids (figure 5) were studied. Steady state, MRF, k-ε turbulent model and periodic and symmetric boundaries were used in liquid phase simulations.

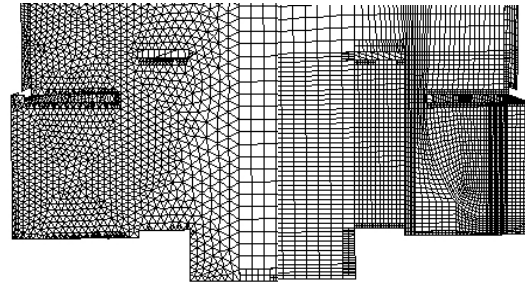


Figure 5: Structured and unstructured grid types.

Tank diameter (mm)	3600
Tank height (mm)	3600
Shaft diameter (mm)	160
Rotor diameter (mm)	825
Rotor bottom clearance (mm)	83
Rotor speed of rotation (rpm)	100/160

Table 1: Geometrical details of the tank.

Mixing time measurements were done by injecting NaCl solution to the impeller area and measuring electrical conductivity of the fluid as a function of time in the upper part of the flotation cell. Mixing time calculations were done with the same geometry and CFD-model than grid dependency calculations. Solver approach was time dependent, unsteady state calculation. In the CFD-model a region in the injection area was adapted and marking solution was patched to it.

#### Grid type dependency and mixing time results

CFD simulation results, consisting of velocity vectors and distributions, pressures in rotor and stator area and turbulence quantities show similar results with both mesh types. No significant grid dependency between structured and unstructured grid types were found. Resultant velocities at two axial levels are shown in figure 6.

Mixing time had good agreement between measured and computed results. Figure 7 shows that significant change of measured conductivity and calculated change of average mass fraction of marker converged.

#### VALIDATION WITH LDV

As a result from grid type dependency model a hybrid grid for a laboratory size Outokumpu flotation cell with unstructured cells in the rotor domain and structured cells in the stator and tank domain was generated. The tank was a cylindrical, unbaffled tank with Outokumpu's rotor-stator flotation device. Computational grid of the rotor-stator area is shown in figure 8. Geometrical details of the tank are given in table 2.

A 60° sector of the tank was modeled with periodic boundaries on the sides of the sector and symmetric boundary on the top of the tank to describe the free surface. Standard wall functions were employed on all wall boundaries of the computational domain. Grid was adapted on the normalized distance to the wall ( $Y^+$ ) during the solution process. Fluent's multiple reference frame steady state approach was used with k-ε turbulence model. Calculation was done in one phase (water).

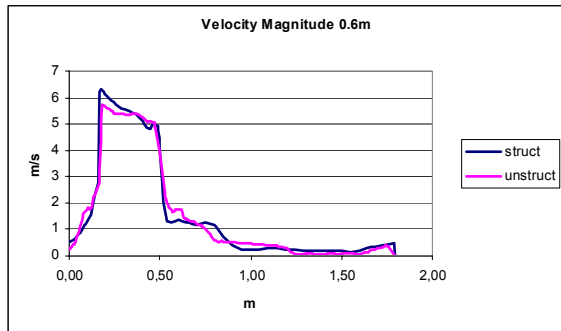
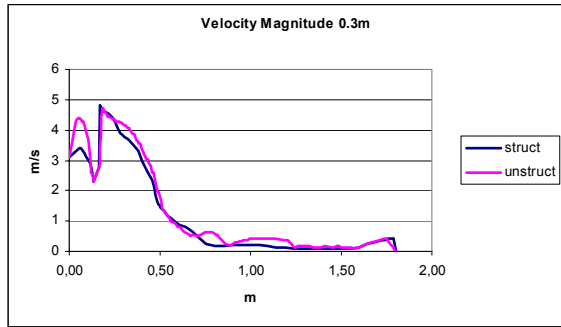


Figure 6: Resultant velocities at two axial levels.

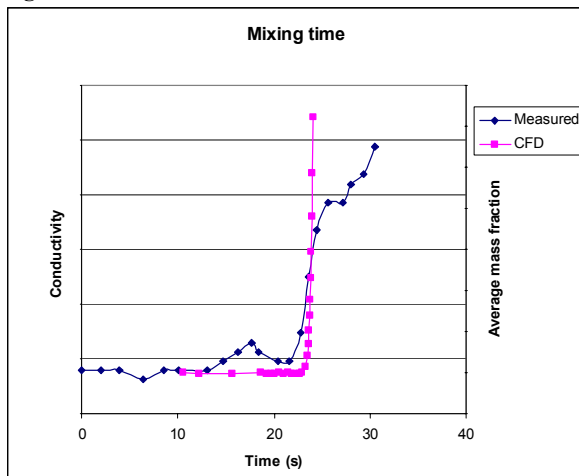


Figure 7: Mixing time results.

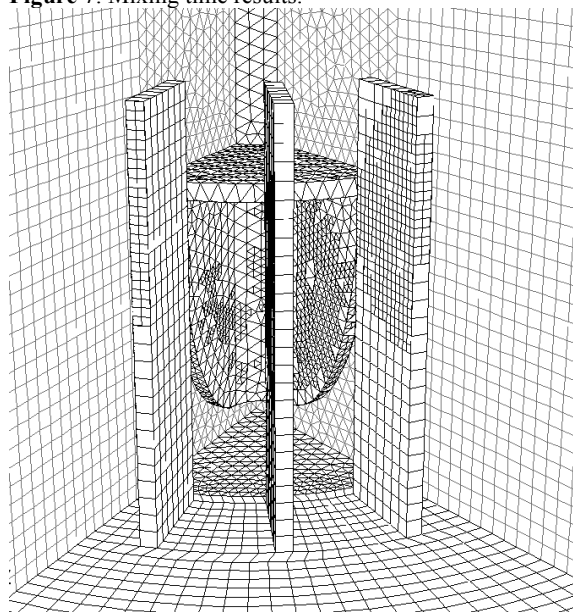


Figure 8: Computational grid of the rotor-stator area.

### LDV results

Results from laboratory size Outokumpu's flotation cell model were compared to Laser Doppler Velocimetry (LDV) measurements done to a similar flotation cell at CSIRO Thermal and Fluids Engineering laboratory. Reasonable agreement is obtained between measured and calculated flow fields. Rotor creates a jet stream in the radial direction towards the cylindrical wall. Two main flows circulates back to the impeller, one through the top side and second from the lower side of the stator. The comparisons of the measured and computed mean velocity components for radial direction as a function of cell height is showed in figures 9 and 10.

Generally, the agreement is good between the measured and computed velocities. Standard k-ε turbulence model suggest lower values than measured in the tank.

Tank diameter (mm)	1070
Tank height (mm)	900
Shaft diameter (mm)	57
Rotor diameter (mm)	270
Rotor bottom clearance (mm)	27
Rotor speed of rotation (rpm)	328

Table 2: Geometrical details of the LDV validation tank.

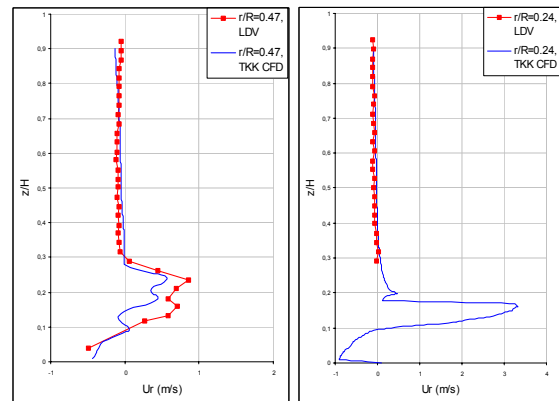


Figure 9: Mean velocity components r/R 0.24 and 0.47.

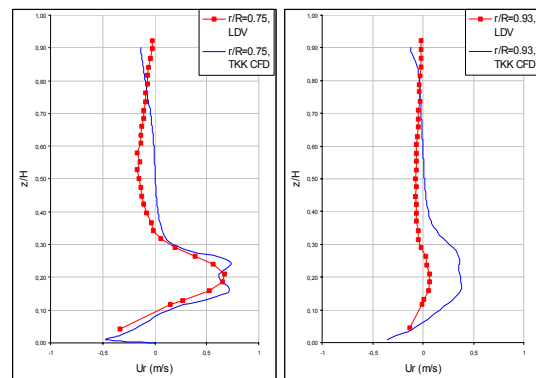


Figure 10: Mean velocity components r/R 0.75 and 0.93.

## VALIDATION WITH POWER MEASUREMENTS

CFD-model was compared with torque moment measurements done by Outokumpu Research. A laboratory size, similar to previous, flotation cell was measured with a moment measuring table. One phase calculations were done with five rotational speeds and fluid was water.

### Power measurement results

In figure 11 is compared calculated and measured values of Outokumpu laboratory size flotation cell power consumption. CFD-model has good agreement with the power consumption in all rotational speeds.

Grid independence was also tested in power calculations. Grid adaptation by  $Y^+$  values was used to improve the quality of the results from the CFD-solution.

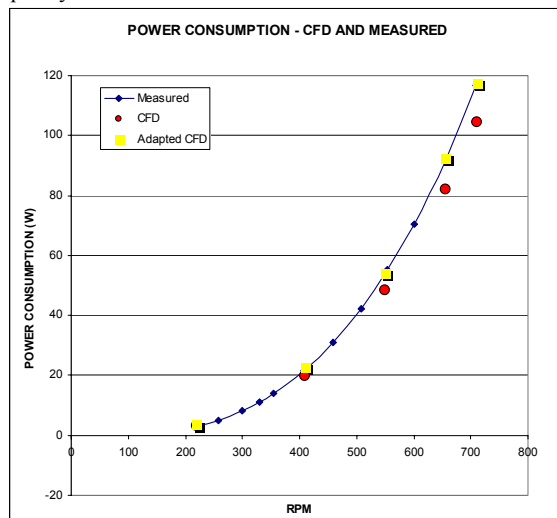


Figure 11: Power consumption.

Similar comparison was also done to industrial size flotation cell. Torque moment was measured straight from the shaft with strain-gage transducer. In that case CFD-model underestimated more the power consumption. Similar moment measuring method is not applicable for laboratory size cells.

## CONCLUSIONS

The complex flow field in the Outokumpu's flotation cell has been studied by CFD. It was proven that converged solution from CFD calculations was grid type independent. Resolution of computational mesh was sufficient when standard wall functions were valid ( $Y^+ = 50-500$ ). Present operation model is to perform grid adaptation, when needed, to get valid  $Y^+$  values.

It was also shown that CFD can be used for predicting mixing time with good accuracy. Different scale of flotation cells caused conflict in power consumption. Solution for this has not been found yet and results can't be exploited at this stage.

The predicted velocity components agreed well with the values obtained from LDV. The standard k- $\epsilon$  model does not predict accurately the k level in the flotation cell compared to measured values.

It was proved that a CFD model with periodicity, hybrid grid and MRF approach can be used for detailed studies on the design and operation of the Outokumpu flotation cell in one phase.

Further studies of numerical modeling of Outokumpu flotation device in two phase (*s,l*) flows are continuing. The work reported is part of a broad national computational fluid dynamics research program.

## ACKNOWLEDGEMENTS

The authors are grateful to Outokumpu Research (Pori, Finland) and AMIRA International Ltd (Melbourne, Australia) for their contribution to this work. AMIRA P9M project's industry partners are acknowledged for their sponsorship. CSIRO Thermal and Fluids Engineering laboratory is acknowledged for the LDV measurements.

## REFERENCES

- MATIS K.A. (Ed.), 1995. Flotation Science and Engineering, Marcel Dekker, Inc., New York, Basel, Hong Kong.
- Fluent Inc. 2002, Fluent manuals.
- Toimi LUKKARINEN 1987, Mineral processing part two, Insinööritieto Oy (In Finnish).
- ZHU, Y., WU J., SHEPHERD I., NGUYEN B. 2002, MineralsModelling of Outokumpu flotation cell hydrodynamics, CSIRO Minerals report DMR-1899.
- VANHANEN T. 2003, Measuring one- and two phase fluids in flotation cells with moment measuring table, Outokumpu Report 03029-ORC-T.
- TIITINEN J., 2003, Numerical modeling of a OK rotor-stator mixing device, poster presentation, ESCAPE-13 symposium, Lappeenranta, Finland.